# Regulation of coordinated muscular relaxation by a pattern-generating intersegmental circuit

Atsuki Hiramoto[1], Julius Jonaitis[2], Sawako Niki[1,3], Hiroshi Kohsaka[1], Richard Fetter[4], Albert Cardona[4,5], Stefan Pulver[2], Akinao Nose[1,6,*]

[1]Department of Complexity Science and Engineering, Graduate School of Frontier Sciences, The University of Tokyo, 5-1-5 Kashiwanoha, Kashiwa, Chiba 277-8561, Japan

[2]School of Psychology and Neuroscience, University of St Andrews, St Mary's Quad, South Street, St Andrews, KY16 9JP, UK

[3]Research Center for Advanced Science and Technology, The University of Tokyo, 4-6-1 Komaba, Meguro-ku, Tokyo 153-8904, Japan

[4]HHMI Janelia Research Campus, Ashburn, VA 20147, USA

[5]Department of Physiology, Development and Neuroscience, University of Cambridge, Cambridge, CB2 3DY, UK

[6]Department of Physics, Graduate School of Science, The University of Tokyo, 7-3-1 Hongo, Bunkyo-ku, Tokyo 113-0033, Japan

[*]Corresponding author

Address correspondence to Akinao Nose at:

Department of Complexity Science and Engineering,

Graduate School of Frontier Sciences, The University of Tokyo,

Kashiwanoha 5-1-5, Kashiwa, Chiba 277-8561, Japan

Tel: 81-4-7136-3919; Fax: 81-4-7136-3919

e-mail: nose@k.u-tokyo.ac.jp

## Abstract

Typical patterned movements in animals are achieved through combinations of contraction and delayed relaxation of groups of muscles. However, how intersegmentally coordinated patterns of muscular relaxation are regulated by the neural circuits remain poorly understood. Here, we identify Canon, a class of higher-order premotor interneurons, that regulates muscular relaxation during backward locomotion of *Drosophila* larvae. Canon neurons are cholinergic interneurons present in each abdominal neuromere and show wave-like activity during fictive backward locomotion. Optogenetic activation of Canon neurons induces relaxation of body wall muscles, whereas inhibition of these neurons disrupts timely muscle relaxation. Canon neurons provide excitatory outputs to inhibitory premotor interneurons. Canon neurons also connect with each other to form an intersegmental circuit and regulate their own wave-like activities. Thus, our results demonstrate how coordinated muscle relaxation can be realized by an intersegmental circuit that regulates its own patterned activity and sequentially terminates motor activities along the anterior-posterior axis.

## Introduction

One of the major goals in neuroscience is to understand how neural circuits regulate movements. Animal movements are generated by sequential contraction and relaxation

of muscles present in different parts of the body[1–3]. While muscle contraction provides the force for moving, timely muscular relaxation is also required for coordinated movements to occur[4–7]. For instance, while a particular muscle (e.g., a limb extensor) is contracted, its antagonistic muscle (e.g., a flexor) must be relaxed. Similarly, muscles in different parts of the body whose simultaneous contraction hinders appropriate body movements must be coordinately contracted and relaxed. Muscle relaxation is thought to be particularly important for fine control of movements required during playing sports and musical instruments[8]. Conversely, deficits in muscle relaxation have been associated with a wide spectrum of movement disorders such as myotonic dystrophy, Parkinson disease and dystonia[8–10].

Muscle contraction ends when transmission from motor neurons (MNs) is terminated, allowing muscle relaxation. Inhibitory motor neurons are present in some invertebrate species and play important roles in tuning muscle relaxation to meet behavioural demands[11–13]. However, termination of MN activity by upstream premotor circuits is also a major mechanism for regulating muscle relaxation. Previous studies in vertebrates and invertebrates have identified a number of premotor interneurons that play roles in patterning motor activities[1–3,14,15]. Although much is known about the timing of muscle contraction, such as how left-right or flexor-extensor alteration is regulated by the premotor circuits, less is known about the cellular and circuit mechanisms of interneuron coordinated muscle relaxation[6,7].

*Drosophila* larval locomotion is an excellent model for investigation of sensorimotor circuits at the single cell level[16–18] (Fig. 1a). The larva has a segmented body and normally moves by forward locomotion. However, when exposed to noxious stimulus to the head, it performs backward locomotion as an escape behavior[16,19,20]. Forward and backward locomotion are symmetric axial movements achieved by

propagation of muscular contraction and relaxation along the body. In both forward and backward peristalses, contraction and relaxation of muscles occur in a segmentally coordinated manner so as to generate a coherent behavioral output[21,22]. Recent studies identified several classes of segmental premotor interneurons that regulate various aspects of larval peristaltic locomotion, including speed of peristaltic propagation, left-right coordination and sequential contraction of antagonistic muscles[5,23–25]. However, none have been shown to be essential for generating the propagation of axial activity. Neither have any been shown to be essential for normal patterns of muscle relaxation during peristaltic locomotion.

Here, we report on the identification of a novel class of segmentally repeated cholinergic interneurons, that we have named Canon (cholinergic ascending neurons organizing their network) neurons, which regulate timely muscular relaxation during larval backward locomotion. Canon neurons show segmentally propagating activities during backward but not forward fictive locomotion at a timing much later than MNs. Optogenetic activation of Canon neurons induced relaxation of body wall muscles, whereas their genetic inhibition severely delayed muscle relaxation. Connectomics analysis (reconstruction of circuit structures in serial electron microscopy (EM) images[26]) revealed that Canon neurons send outputs to a large number of interneurons, but are particularly strongly connected to a group of first-order inhibitory premotor interneurons. Taken together, our results suggest that Canon neurons regulate muscle relaxation by providing delayed excitation to inhibitory premotor interneurons. We also found that Canon neurons in abdominal neuromeres connect with each other to form an intersegmental network that regulates their own propagating activities. Thus, our results demonstrate how coordinated muscle relaxation can be regulated by the action of a pattern-generating intersegmental circuit.

## Results

### Canon neurons are ascending interneurons active during backward but not forward locomotion.

Neurons that regulate specific motor patterns are often recruited in a manner related to the pattern. To identify neurons related to backward locomotion, we searched for interneurons showing backward-specific activity propagation by calcium imaging. We identified among the neurons targeted by *R91C05-Gal4* a novel class of segmentally repeated interneurons that we termed 'Canon' due to their distinctive morphological and functional features. These neurons showed wave-like activity propagation in the backward direction but not in the forward direction (Fig. 1b, Supplementary Fig. 1a, b, and Supplementary Movie 1). Since *R91C05-Gal4* only targets Canon neurons in abdominal neuromeres A3-A5, we also generated an independent Gal4 line, *Canon-spGal4*, which drives expression in Canon neurons in A1-A6 neuromeres (Supplementary Fig. 1c). To study the timing of Canon neuron activity relative to MNs, we conducted simultaneous calcium imaging of Canon neurons and aCC MNs (Fig. 1c, d, Supplementary Fig. 1d, e, and Supplementary Movie 2)[27,28]. Canon neurons were activated after aCC MNs in the same neuromere and at a similar timing to aCC MNs in neuromeres 2–3 segments more anterior suggesting possible roles in the termination of segmental motor activity (Fig. 1d and Supplementary Fig. 1e). The dual calcium imaging also confirmed that Canon neurons were activated during fictive backward but not forward locomotion (Fig. 1c).

We next studied the neurite morphology and neurotransmitter phenotype of Canon neurons. We generated single-cell clones of Canon neurons using the MultiColor FLP-Out (MCFO) method[29], and studied axon and dendrite extension of individual Canon

neurons (Fig. 1e, f). We also used the DenMark technique[30] to identify pre- (visualized with Syt-GFP) and post-synaptic (visualized with the DenMark marker) sites (Supplementary Fig. 1i). These analyses revealed characteristic morphological features of the Canon neurons, as detailed below. The cell bodies of Canon neurons were located in a ventrolateral region of the VNC (Fig. 1f) and extended an axon initially to the contralateral dorsal neuropil via the anterior commissure (Supplementary Fig. 1f), and then anteriorly to the T2 neuromere (Fig. 1e). The ascending axons sent collaterals in each of the two to three neuromeres anterior to the cell body and arborized presynaptic terminals in the dorsal neuropil, which are known to contain MN dendrites. Canon neurons expressed choline acetyltransferase (ChAT), a marker for cholinergic neurons, but not vesicular glutamate transporter (vGluT)[31], a marker for Glu, or GABA, (Fig. 1g and Supplementary Fig. 1g, h), suggesting that Canon neurons are cholinergic and most likely excitatory. To summarize, Canon neurons are segmental ascending interneurons activated after MNs during backward locomotion.

## Optogenetic activation of Canon neurons induces muscular relaxation.

Canon neurons are activated after MNs in each neuromere and send information via the ascending axons to anterior neuromeres, (i.e. in the opposite direction to backward propagation). Thus, Canon neurons may play roles in shutting down MN activities in anterior neuromeres during backward locomotion. To study this, we conducted gain-of-function experiments via optogenetic activation of Canon neurons. Since *R91C05-Gal4* and *Canon-spGal4* drove expression not only in Canon neurons but also in other neurons, including Wave neurons whose activation is known to induce backward locomotion and other escape behaviors[20], they were not suitable for the gain-of-function analyses (Supplementary Fig. 1a, c, and Supplementary Fig. 2a, b). However, we found

147 that *R91C05-LexA* drove expression only in Canon neurons in neuromeres A1 to A3 (Fig.
148 2a) and used this for the gain-of-function analysis. We expressed CsChrimson, a red-
149 shifted Channelrhodopsin[32], in Canon neurons, and optogenetically activated these
150 neurons with short (5 sec) light pulses. When photostimulation was applied to control
151 larvae, all animals continued forward locomotion since they are insensitive to red light.
152 In contrast, when light was applied to experimental larvae undergoing forward
153 locomotion, a majority of them (8 out of 10) halted and showed visible muscle relaxation
154 (Fig. 2b and Supplementary Movie 3). We quantified the phenotype by counting the
155 number of forward peristalses during light application and found it to be significantly
156 reduced in the experimental group (Fig. 2c). These results are consistent with the idea
157 that Canon neurons induce relaxation of body muscles.
158
159 **Canon neurons are required for proper muscular relaxation**.
160 We next studied whether Canon neurons are required for muscular relaxation during
161 backward locomotion by conducting loss-of-function experiments. We expressed Kir2.1
162 (inwardly-rectifying potassium channel)[33] in Canon neurons to suppress baseline
163 excitability and observed muscle dynamics in dissected larvae undergoing spontaneous
164 forward and backward peristalses (by visualizing muscles with *Mhc > GFP*[34]; Fig. 3a).
165 We found that the muscular relaxation was disrupted and peristalses duration were
166 prolonged during backward peristalses, but not forward peristalses, when Canon
167 neurons' activity was suppressed (Fig. 3b, c, and Supplementary Movie 4).
168 To examine the phenotype more closely at the cellular level, we focused on a
169 ventral longitudinal (VL) muscle (muscle 6) in segment A3 and measured the change in
170 length of the muscle during peristalses (Fig. 3d). We then obtained the maximum speed
171 of muscular relaxation and contraction and the duration of muscular contraction, and

compared the values between forward and backward peristalses and between the control and experimental groups (Fig. 3e-j). The quantification revealed that maximum relaxation speed was dramatically decreased and the duration of muscular contraction was prolonged during backward but not forward peristalses when Canon neuron function was inhibited. The result further supports the notion that Canon neurons regulate relaxation of muscles during backward peristalses. There was also a slight decrease in contraction speed during backward peristalses when Canon neurons were silenced (Fig. 3h). Since Canon neurons are not active during the muscle contraction phase, this is likely an indirect consequence of the delayed muscular relaxation: it is well known that sensory feedback modulates the speed of locomotion, and it has been suggested that completion of muscular contraction and relaxation in one segment may activate the premotor circuits in the next segment via sensory feedback[34].

The above experiments were conducted using *Canon-spGal4*, which targets Wave neurons in addition to Canon neurons, instead of the Canon-specific *R91C05-LexA*, since LexAop constructs suitable for the loss-of-function experiments were not available. Previous studies have shown that Wave neurons are not active during spontaneously occurring fictive locomotion and thus are unlikely to regulate the relaxation of muscles during peristalses. However, to further exclude the involvement of Wave neurons, we studied the effects of inhibiting Wave activity by using an independent Wave-specific Gal4 driver (*MB120B-spGal4*). No abnormality was seen in the muscular contraction or relaxation during forward and backward peristalses (Supplementary Fig. 2c, d). Taken together, these results indicate that Canon neurons are required for proper muscular relaxation during backward peristalses.

**Canon neurons receive inputs from command systems for backward**

**locomotion.**

To further study how Canon neurons regulate muscular relaxation during backward locomotion, we elucidated the circuit structure around Canon neurons using reconstructions from a serial section transmission electron microscopy (ssTEM) image data set of an entire first instar larval CNS[35]. Since premotor circuits were the likely targets of Canon neurons and previous studies comprehensively reconstructed 1st-order premotor interneurons in neuromere A1[26], we started reconstruction of Canon neurons in neuromeres A2 and A3, which arborize presynaptic sites in neuromere A1. We first uniquely identified Canon neurons in the existing ssTEM reconstruction based on the morphological features obtained from the single-cell MCFO clones (Fig1. e, f), and found them annotated as 'A18g' (Fig. 4a). We then extended the reconstruction to upstream and downstream synaptic partners of the Canon neurons (Figs. 4-6 and Supplementary Figs. 3-5). The upstream neurons with the largest synaptic occupation of the Canon neurons were: (1) thoracic descending neurons (ThDNs), (2) A27l interneurons, and (3) Canon neurons themselves (Fig. 4b-f and Supplementary Fig. 3a, b). ThDNs, descending neurons present in the thorax, are major components of the downstream circuits of mooncrawler descending neurons (MDNs), command neurons of backward locomotion located in the brain (Fig. 4f)[36]. A27l neurons, segmental interneurons present in the VNC, are major downstream partners of ThDNs[36]. In addition, Canon neurons receive direct inputs from MDNs. Thus, Canon neurons receive large synaptic inputs directly or indirectly from MDNs (Fig. 4f and Supplementary Fig. 3b). These results suggest that Canon neurons are recruited during backward locomotion by the backward command system. In addition to the MDN command system, Canon neurons receive major inputs from Canon neurons in other neuromeres and thus form a bidirectionally connected circuit composed of segmental homologues (hereafter called Canon-Canon

network) as will be detailed below. Thus, two major sources of inputs to Canon neurons are the MDN command system and the Canon-Canon network (Fig. 4f).

## Canon neurons provide outputs to inhibitory premotor circuits

Major downstream partners of the Canon neurons include: (1) first-order premotor interneurons A06a, A06c, A31d, and A31k, (2) second-order premotor interneurons A02l and GVLIs, (3) Canons themselves, and (4) intersegmental neurons located in the thorax or subesophageal zone (SEZ) named post Canon neuron 04, 23, and 05 (Fig. 5, Supplementary Fig. 3d, and Supplementary Fig. 4). Consistent with the notion that Canon neurons regulate muscular relaxation, all of the four first-order premotor interneurons appear to be inhibitory. A06a, A06c and A31k were previously identified as putatively inhibitory since they express GABA[37,38]. Another downstream premotor neuron A31d was putatively GABAergic because it belongs to the same lineage as A31b and A31k - premotor interneurons previously identified as GABAergic - and shares morphological characteristics to these neurons[25,37,38]. We confirmed that the premotor interneuron A06c, one of the strongest postsynaptic partners of Canon neurons was GABAergic (Supplementary Fig. 4a-c). We also verified that Canon neurons form synapses with A06c neurons using the sybGRASP method (Supplementary Fig. 4d, e). Each of these four classes of premotor interneurons in A1 received inputs from two Canon neurons located in neuromeres A2 and A3 and send outputs to MNs, most of which innervate longitudinal muscles located in the segments A1 and A2 (Fig. 5h). This circuit configuration predicts Canon neurons provide late-phase and prolonged inhibition to MNs during backward locomotion (see Discussion).

The second-order premotor neurons A02l and GVLI are segmentally repeated local interneurons (Fig. 5d, e, g, and Supplementary Fig. 3d)[17,37,39,40]. GVLIs not only

247 receive inputs from Canon neurons directly but also indirectly via A02l neurons,
248 suggesting that these two second-order premotor neurons function in closely related
249 circuits (Fig. 5h). A previous study showed GVLI neurons are glutamatergic neurons
250 whose optogenetic activation elicits muscular relaxation[39]. While GVLIs formed direct
251 synaptic contacts with MNs, a majority of the downstream targets were first-order
252 premotor interneurons including the premotor interneuron, A31d, which is also a direct
253 target of Canon neurons (Fig. 5h). GVLIs show activities during fictive forward[39] and
254 backward (this study, Supplementary Fig. 4f) locomotion. The fact that activation of
255 GVLIs, like that of Canon, induces muscular relaxation suggests that Canon neurons
256 induce muscular relaxation in part by activating GVLIs. To further study the role of GVLIs,
257 we conducted transient loss-of-function behavior analyses using the light-gated anion
258 channel, GtACR1[41], which was not available in the previous study[39]. Upon optogenetic
259 inhibition, the larvae underwent rapid abdominal contraction (Fig. 5j). This suggests that
260 GVLIs inhibit inappropriate contraction of muscles during locomotion and corroborates
261 the role of GVLIs in the regulation of muscular relaxation. To summarize, major
262 downstream targets of Canon neurons are Canon-Canon circuits and inhibitory premotor
263 circuits including the first- and second order premotor interneurons, through which Canon
264 neurons appear to induce muscular relaxation (Fig. 5h).
265
266 **Canon-Canon network regulates its own intersegmentally propagating**
267 **activities.**
268 As mentioned above, Canon neurons connect bidirectionally with other Canon neurons
269 (Fig. 6a-e and Supplementary Fig. 3b, d). We first noticed connections between Canon
270 neurons in segments A2 and A3: the right Canon neuron in A2 forms synapses with the
271 right Canon in A3 bidirectionally, in the bundle consisting of Canon neurons' ascending

axons. We extended the reconstruction to Canon neurons in neuromeres A4 and A5 and found bidirectional synaptic connections between all combinations of the four Canon neurons in A2-A5 (Supplementary Fig. 5). No synapses were seen between the right and left Canon neurons.

To study the roles of the Canon-Canon network in generating the wave-like activity of Canon neurons, we conducted loss-of-function analyses of the outputs of Canon neurons. In this experiment, we inhibited Canon neurons' chemical transmission by expressing tetanus toxin (TeTxLC)[42] and observed the Canon neurons' activity using calcium imaging. In this condition, inputs from other upstream neurons to the Canon circuits are not perturbed (Fig. 6e, f). If the pattern of Canon neurons' activity is solely generated by upstream neurons other than Canon neurons, the Canon neurons should show wave-like activity even if Canon neuron synapses are suppressed. However, if synaptic transmission between Canon neurons is required for the wave-like activity, it should be disrupted in this condition. We found that the latter was the case (Fig. 6g-i). When synaptic transmission by Canon neurons was inhibited, wave-like activity in Canon neurons was initiated but often failed to propagate all the way to the posterior end. This result suggests that synaptic transmission between Canon neurons is necessary for their own wave-like activity.

It is important to note that propagation of excitatory drive appears to be normal in all experimental animals (*Canon* > *TeTxLC*): the wave of muscular contraction propagated to the posterior ends in dissected larvae (Supplementary Fig. 6a-c). Thus, inhibition of synaptic transmission by Canon neurons specifically inhibits the propagation of their own activity crucial for muscular relaxation but leaves the propagation of the excitatory drive intact.

## Discussion

Our study identified a new class of premotor interneurons, the Canon neurons, that regulate muscular relaxation, and revealed their cellular-level circuit structure, including the upstream backward command neurons and downstream inhibitory premotor circuits extending from the brain to the muscles. Moreover, we found that Canon neurons form synapses with each other to constitute a self-regulating circuit. Our results suggest that the Canon-Canon network is important, not only as an actuator of muscular relaxation in each segment, but also as the pattern generator of its own propagating activity during backward locomotion.

### Regulation of premotor inhibition and muscular relaxation

For animal movements to occur in a patterned and coordinate manner, timing of not only muscle contraction but also muscle relaxation must be precisely controlled. In locusts, inhibitory GABAergic motor neurons have been shown to regulate muscle performance to optimize behavioral performance in a variety of contexts including postural control, predatory strikes, and escape movements[12,43]. Similarly, in the nematode *C. elegans*, patterns of spiking in excitatory and inhibitory motor neurons regulate muscle contraction and relaxation[13,44]. Motor neuron activity is also dependent on the activity of excitatory and inhibitory interneuron populations. While previous studies have identified a number of interneurons and circuits that regulate muscle contraction in various model systems, neural circuit mechanisms underlying the timing of muscle relaxation are less well explored[6–8]. Here, we revealed crucial roles played by Canon neurons in the regulation of muscle relaxation during backward locomotion of *Drosophila* larvae. The following evidence points to the role of Canon neurons in muscle relaxation, not contraction. First, Canon neurons are activated much later than the downstream MNs. Calcium imaging

showed that Canon neurons are active later than MNs in the same neuromere and at a similar timing as MNs in the next or third neuromere during fictive backward locomotion (corresponding to a phase delay of 1-2 neuromeres; Fig. 1d and Supplementary Fig. 1e). Additionally, EM reconstruction shows that Canon neurons (via premotor interneurons) connect to MNs in the next or third neuromere, in the opposite direction to backward wave propagation (generating a delay of 1-2 neuromeres; Fig. 5). Taken together, Canon neurons are activated with a delay corresponding to propagation in 2-4 neuromeres to their target MNs during fictive locomotion. This late onset of Canon activities implies roles in muscle relaxation not excitation. Second, optogenetic activation of Canon neurons induces muscle relaxation in the larvae (Fig. 2b, c). Third, loss-of-function of Canon neurons impaired muscle relaxation during backward peristalses of dissected larvae (Fig. 3). This indicates that orchestrating muscle relaxation pattern during backward waves is an active process requiring the activity of Canon neurons. Finally, Canon neurons target a number of premotor interneurons, which can potentially inhibit MNs. Since Canon neurons are cholinergic and thus likely excitatory, their activation, and in turn, downstream premotor interneurons, can terminate MN activity and thus induce muscle relaxation (Fig. 5). Taken together, our results reveal a circuit motif regulating muscle relaxation consisting of a second-order excitatory premotor interneuron (Canon) and a group of downstream inhibitory premotor interneurons, including both first-order (such as A06c) and second-order (such as GVLI) premotor neurons. While our results are consistent with this model for Canon neuron function on the time scales of activation studied, it is important to note that Canon neurons also connect to a large number of other interneurons that are not premotor inhibitory cells. This suggests that Canon neurons may also have additional functional roles mediated by other downstream partners.

Larval musculature consists of two groups of antagonistic muscles: longitudinal muscles that contract the body along the anterior-posterior axis, and transverse muscles that contract the body circumferentially[45]. These two groups of antagonistic muscles are activated at different times with the longitudinal muscles contracting earlier [21,46] during peristalses. Premotor interneurons immediately downstream of Canon neurons described above provide inhibitory inputs largely to longitudinal muscles rather than transverse muscles, suggesting that Canon neurons may primarily regulate the relaxation of a specific functional type of muscle within the neuromuscular system (Fig. 5h).

## Circuits mediating early- and late-phase motor inhibition

Previous studies in larvae identified several classes of segmental premotor interneurons whose optogenetic activation induces muscle relaxation, including the first-order premotor interneurons PMSI and iIN, and second-order premotor interneurons GDL[5,24,25,46]. Of these, GDL and iIN neurons are activated earlier than their target MNs and regulate the timing of muscular contraction rather than relaxation either via disinhibition (GDL) or by acting as a delay line (iIN). In contrast, PMSI neurons, like Canon, are activated later than their target MNs and regulate the duration of MN activities and speed of locomotion. Thus, PMSIs could potentially play roles in the regulation of muscle relaxation although this possibility has not been directly addressed.

PMSIs together with other inhibitory premotor interneurons are activated by the second-order premotor interneurons, Ifb-Fwd and Ifb-Bwd neurons, during forward and backward locomotion, respectively[24]. Ifb-Fwd and Ifb-Bwd neurons are active at a similar timing to MNs in the same neuromere and provide excitation to PMSIs and other shared downstream premotor interneurons in the adjacent neuromere behind the motor

propagation, which in turn provide inhibitory inputs to MNs innervating longitudinal muscles (L-MNs) and excitatory inputs to MNs innervating the antagonistic and later-activating transverse muscles (T-MNs, Fig. 7 and Supplementary Fig. 7a, b). Thus, during backward locomotion, timing of the activation of inhibitory premotor interneurons (and ensuing muscular relaxation) appears to be regulated via at least two pathways, one including Ifb-Bwd neurons and providing activation at a relatively early phase (~1 neuromere behind the wave front) and the other including Canon neurons and providing activation at a late phase (2-4 neuromeres behind the wave front; Fig. 7). It would be interesting to study in the future whether there exists a counterpart of Canon neurons during forward locomotion that mediates a late-phase inhibition.

Interestingly, Ifb-Bwd and Canon neurons provide inputs to almost non-overlapping sets of inhibitory interneurons, suggesting that dedicated premotor interneurons mediate early- versus late-phase motor inhibition (Supplementary Fig. 7c). A31k is the only downstream inhibitory premotor neurons common to Canon and Ifb-Bwd neurons. Activity of the A31k neuron lasts much longer than that of A02e (a PMSI) which is only innervated by Ifb-Bwd neurons, consistent with the idea that Ifb-Bwd and Canon neurons provides early- and late-excitation to this and other downstream neurons, respectively (Supplementary Fig. 7d-h).

## Possible roles of Canon neurons in the maintenance of relaxed state of muscles

Inhibition mediated by Canon neurons is not only later but also likely longer compared to that mediated by Ifb-Bwd neurons, since the target premotor interneurons in each neuromere receive inputs from Canon neurons in two consecutive neuromeres. The long duration of Canon-mediated activation suggests that it is present even after MN activity

ceases. Thus, Canon-mediated late-phase inhibition may play roles not only in the process of muscular relaxation but also maintenance of the relaxed state after movement, which might be important to inhibit inappropriate contraction induced by self-generated sensory signals[47]. In *Drosophila* larvae, it is known that muscle contraction activates a group of proprioceptors, including the dorsal and ventral bipolar dendrite md neurons (dbd and vbd, respectively[23,48]), which provide direct and indirect excitatory outputs to MNs[23]. These proprioceptive signals could inappropriately activate MNs and induce muscle contraction behind the peristaltic wave. Canon neurons may suppress such inappropriate muscular contraction by providing prolonged inhibitory inputs to MNs. The results of the transient inhibition of GVLIs, a strong downstream target of Canon neurons, are consistent with this idea. When GVLI activity was optogenetically inhibited during locomotion, the larvae immediately and strongly contracted their muscles in an abnormal fashion and ceased locomotion. One possibility is that MNs receive tonic or phasic excitatory inputs when not being recruited during locomotion, which would interfere with the execution of the locomotor waves and have to be continuously suppressed by inhibitory signals from GVLIs. Interestingly, GVLIs receive strong inputs not only from Canon neurons but also from proprioceptive sensory neurons, dbd and vbd. A02l, another second-order premotor interneuron downstream of Canon, also receive inputs from the dbd proprioceptor. Thus, GVLIs and A02l neurons may regulate muscular relaxation by integrating signals from the central pattern generating circuits (via Canon neurons) and from proprioceptive feedback (via dbd and vbd, Fig. 5i).

## Canon-Canon network regulates its own intersegmentally propagating activities

Our results showed that Canon neurons regulate not only muscle relaxation but also their

own intersegmentally propagating activities. Segmentally repeated Canon neurons bidirectionally connect with each other by forming a bundle of axons (Fig. 6a-e). When synaptic transmission in the Canon-Canon network was inhibited, segmentally propagating activity of Canon neurons was often interrupted (Fig. 6f-i). It should be noted that in the absence of transmission by the Canon-Canon network, waves of muscle contraction propagated normally in all peristalses we observed (Supplementary Fig. 6). Thus, the Canon-Canon network constitutes a circuit specialized for generating the pattern of muscular relaxation. However, the activity of Canon neurons should also be under the influence of the earlier activating excitatory CPGs since Canon activities and muscle relaxation must occur in phase with contraction of muscles. Indeed, calcium imaging showed that propagating activity of Canon neurons is in phase with that of earlier activating MNs (Fig. 1c, d and Supplementary Fig. 1e). Thus, the Canon-Canon network appears to function as a sub-circuit or smaller pattern generating circuit that functions within a larger CPG, as proposed in other systems[1,3].

Canon neurons are activated later than MNs in the same neuromere with a lag of one to two neuromeres (Fig. 1c, d and Supplementary Fig. 1e). In contrast to Canon neurons, the activities of Ifb-Fwd and Ifb-Bwd neurons, which also mediate motor inhibition, occur at a similar timing as MNs in the same neuromere and are likely under direct influence of the CPGs driving motor excitation. Delay appropriate for motor inhibition is realized in the Ifb-Fwd and Ifb-Bwd pathway by projecting an intersegmental axon in an opposite direction to the motor wave. Similarly, Canon neurons send intersegmental axons to connect with premotor neurons in neuromeres behind the motor wave, so as to activate the downstream neurons with a delay corresponding to one or two neuromeres compared to the wave front. However, to generate even longer delays in muscle relaxation, Canon neurons may have evolved to form a pattern generating

447 circuit which is capable of generating delayed propagating activities distinct from the
448 excitatory activity propagation.

449 How the Canon-Canon network generates propagating waves of activity remains
450 to be determined. We found that Canon neurons receive strong inputs from ThDNs
451 neurons which in turn are activated by MDNs, command-like neurons for backward
452 locomotion. The combination of these descending inputs, Canon-Canon signaling and
453 some other signals from the excitatory CPGs may generate the delayed propagating
454 activity for muscle relaxation. Further exploration of the connectome and circuit
455 mechanisms underlying the delayed propagation will be important future goals. It will
456 also be interesting to study if similar circuit motifs as the Canon-Canon network regulate
457 the timing of muscle relaxation in other invertebrate and vertebrate systems. Prolonged
458 muscle contraction and delayed relaxation, as observed in larval preparations with
459 inhibited Canon function, is a common symptom found in various human movement
460 disorders[8–10]. Further investigation of Canon-Canon network and related circuits in other
461 species may shed new light on our understanding of the control of muscle relaxation in
462 health and disease.

463

464 **Figure legends**

465 **Fig. 1 Activity and anatomy of Canon neurons.**

466 (a) (Left) A scheme of a larval body which is segmented into T1-3 and A1-9(top). A
467 scheme of a dissected larva, body-wall muscles, and the CNS (bottom). A CNS is also
468 segmented and MNs on located in each neuromere sends outputs to muscles located
469 on corresponding segment. (Right) Larval peristaltic behavior is generated by the
470 propagation of muscular contraction (red) and delayed relaxation (blue) (left) which are
471 induced by propagation of activity of MNs (red) (right). (b) Canon neurons in A3-A5

neuromeres show propagating activity in the backward direction. (c) Simultaneous imaging of A3 Canon neuron (magenta) and A3-A5 aCC MNs (blue). Backward (bwd) and forward (fwd) fictive waves are indicated by arrows in (b, c). (d) Linear phase plot of activity peaks in an A3 Canon neuron (magenta) and A3-A5 aCC MNs (blue) during backward waves. Each of the two horizontal lines represents an individual preparation. The timing of the activity peaks in each neuron relative to the phase of backward peristalses were plotted. Phase 0 is initiation of activity of A2 Canon neuron, while Phase 1 is peak of activity of A6 Canon neuron. $n$ = 19 waves from two larvae. (e, f) Morphology of single-cell clones of Canon neurons in A3 (top) and in A4 (bottom) obtained by MCFO. Dotted lines indicate segmental borders identified by the Fasciclin2 (Fas2)-positive TP1 tract[49]. (e) Dorsal view, (f) Anterior view reconstructed from the region shown by a white box in (e). (g) A focal plane showing that presynaptic sites of Canon neurons visualized by the expression of a presynaptic marker Syt-GFP (green) are also positive for ChAT (magenta, arrows). Scale bars in (e, f), 50 µm. Scale bar in (g), 5 µm.

**Fig. 2 Activation of Canon neurons induces muscular relaxation.**

(a) Expression of CsChrimson driven by *R91C05-LexA*. Note that the expression is only seen in Canon neurons. (b) Time-lapse images (top) and stack images (bottom) of control (left, ATR-) and experimental (right, ATR+) larvae during optogenetic perturbation. The experimental larva stopped immediately with its body relaxed when exposed to red light. 0 sec indicates the onset of light stimulation. (c) Quantification of the number of forward peristalses during the first 2 seconds of light stimulation. $n$ = 10 larvae in each group. Eight out of ten larvae in the experimental group halted with their muscles relaxed upon photo-stimulation, while no control larvae stopped locomotion. $^{**}p = 4.29 \times 10^{-3} < 0.01$, the two-sided Fisher exact test with the Holm method. Scale

bars, 50 μm (a) and 1 mm (b).

**Fig. 3 Canon neurons are required for proper muscular relaxation during backward peristalses.**

(a) An image of body-wall muscles visualized by expression of *MhcGFP*, focusing on ventral muscles in segments A2-A3. The white solid line indicates the length of muscle 6 and the white dotted line indicates the location used to make the kymographs shown in (b, c). (b, c) Kymographs showing movement of the ventral muscles in dissected control (Gal4 negative condition) (b) and *Canon-spGal4 > UAS-Kir* (c) larvae. Bars on the right side of each kymograph indicate the duration of backward (B) and forward peristalses (F), respectively. Note elongated duration of backward peristalses in the experimental animal. (d) Plots of muscular length (cyan line) and its time differential (blue line) during forward (top) and backward peristalses (bottom). Magenta and green points indicate the time point when relaxation (magenta) and contraction (green) speed is maximum, respectively. (e-h) Comparison of the maximum muscular relaxation (e, f) and contraction (g, h) speed during forward and backward peristalses. (I, j) Comparison of duration of muscular contraction during forward (i) and backward (j) peristalses. $n$ = 25 forward and 28 backward peristalses in three control larvae and 46 forward and 15 backward peristalses in three experimental larvae. $^{****}p = 1.42 \times 10^{-7} < 0.0001$ (f), $^{****}p = 4.32 \times 10^{-5} < 0.0001$ (h), $^{**}p = 2.70 \times 10^{-3} < 0.01$ (j), n.s.; not significant: $p > 0.05$, the two-sided Mann-Whitney U test. Scale bars in (a, b), 500 μm.

**Fig. 4 Upstream circuits of Canon neurons.**

(a) EM reconstructed of Canon neurons in neuromeres A2 and A3. (b) A bar graph of postsynaptic occupation of A2-A3 Canon neurons. Major partners (occupying more than

5 % of total postsynapses) are shown. (c) An EM image showing synapses between ThDN neuron (presynapse, orange) and A2 Canon neuron (postsynapse, light blue). White arrows indicate T-bars. (d, e) Dorsal (d) and anterior view (e) of reconstruction images of ThDNs (orange) and A2 Canon (blue) neurons. Triangles indicate the midline. (f) A diagram of connectivity from MDN to Canon neurons. Arrows with filled heads indicate cholinergic synapses while arrows with empty heads indicate synapses with unidentified neurotransmitter. The bar indicates inhibitory outputs. Numbers next to the lines show the number of synapses. Scale bar (c), 50 nm.

**Fig. 5 Downstream circuits of Canon neurons.**

(a) A bar graph showing presynaptic occupation of A2-A3 Canon neurons. Major partners (occupying more than 2.5 % of total presynapses) are shown. (b, c) Dorsal view (b) and anterior view (c) of EM reconstructed A06c and Canon neurons. (d, e) Dorsal (d) and anterior (e) view of reconstruction images of GVLI and Canon neurons. (f, g) EM images showing synapses between Canon (cyan) and A06c (f, magenta) or GVLI (g, purple) neurons. White arrows indicate T-bars. (h) A circuit diagram from Canon neurons to muscles. Grey dotted lines indicate boundaries of neuromeres. Arrows with triangle heads indicate excitatory synaptic connections, lines with bar heads inhibitory synaptic connections and those with diamond-shaped heads glutamatergic synapses. (i) GVLI and A02l neurons receive inputs from Canon neurons and proprioceptors. (j) Optogenetic inactivation of GVLI neurons in a *R26A08-Gal4 > GtACR1* larva induces rapid muscular contraction. 0.0 sec indicates onset of stimulation. $n$ = 10 larvae in both control (ATR negative condition) and experimental groups. Nine out of ten experimental larvae showed rapid abdominal contraction upon photo-stimulation, while all control larvae were unaffected. Scale bars (f, g), 500 nm.

**Fig. 6 Canon-Canon network regulates its own wave-like activity.**

(a, b) EM reconstructed Canon neurons in A2 and A3. Note that these neurons form a bundle of ascending axons. Dorsal (a) and anterior (b) view. (c, d) EM images showing bidirectional synapses between Canon neurons. White arrows indicate T-bars. (e, f) Schemes of Canon-Canon networks in control (e) and *Canon* > *TeTxLC* (f) larvae. Canon neurons connect with each other via synapses present in their ascending axons. TeTxLC disrupts Canon-Canon transmission but leaves input from other upstream neurons intact. (g, h) Activity propagation among Canon neurons in control (g) and *Canon* > *TeTxLC* (h) larvae. Arrows with solid lines indicate complete waves, while those with dotted lines indicate incomplete waves. (i) A cross table showing the number of complete and incomplete waves in the control (-TeTxLC) and *Canon* > *TeTxLC* (+TeTxLC) larvae. The number of incomplete waves is significantly increased in the experimental group. $n$ = 19 waves in four control larvae and 27 waves in seven experimental larvae. *** $p = 3.56 \times 10^{-4} < 0.001$, chi-squared test. Scale bars (c, d) indicate 500 nm.

**Fig. 7 A model of early- and late-phase motor inhibition mediated by Ifb-B and Canon neurons during backward locomotion.**

When the wave front reaches the segment (n), Ifb-Bwd neurons in segment (n) and Canon neurons in segment (n-1) and segment (n-2) are activated. Ifb-Bwd and Canon neurons in turn activate inhibitory premotor neurons (inPMN) innervating L-MNs in segment (n-1) and in segments (n-2) to (n-4), respectively, via their ascending axons. Ifb-Bwd neuron activates excitatory premotor neurons (ePMN) that innervate T-MNs. Neurons outlined by dotted or solid lines indicate inactive or active neurons, respectively. Arrows with filled heads indicate excitatory synapses while those with bar heads indicate

572 inhibitory outputs.

573

574 **Methods**

575 ***Drosophila melanogaster* strains**

576 Third-instar larvae of the following fly strains were used for all functional and histological
577 experiments. *y*[1] *w*[1118] (Bloomington *Drosophila* Stock Center (BDSC), #6598), *R91C05-Gal4*
578 (BDSC, #40578), *R26A08-Gal4*[39] (BDSC, #49153), *RRa-Gal4*[50] (gift from Dr. Miki Fujioka), *UAS-*
579 *GCaMP6s*[51] (BDSC, #42746), *UAS-CD4::GCaMP6f*[24], *UAS-TeTxLC*[42] (BDSC, #28838), *UAS-*
580 *Kir2.1::EGFP*[33] (BDSC, #6596), *UAS-GtACR1*[36,41] (gift from Dr. Chris Doe), *UAS-CD4::tdGFP*[52]
581 (BDSC, #35836), *UAS-DenMark, UAS-syt::GFP/CyO; D/TM6C* (*UAS-TLN-21*)[30] (gift from Dr.
582 Bassem A. Hassan), *MCFO4*[29] (BDSC, #64087), *MCFO6*[29] (BDSC, #64090), *R91C05-LexA*
583 (BDSC, #61629), *LexAop-CsChrimson::mVenus*[32], (BDSC, #55136), *sybGRASP* (*lexAop-nSyb-*
584 *spGFP1-10, UAS-CD4-spGFP11*)[53] (BDSC, #64315), *MhcGFP*[34] (gift from Dr. Cynthia L.
585 Hughes), *Canon-spGal4* (A combination of *R91C05-Gal4.AD* (BDSC, #70979) and *VT019059-*
586 *Gal4.DBD* (BDSC, #71731)), *MB120B-spGal4*[20], *A06c-Gal4* (A combination of *R24A05-Gal4*
587 (BDSC, #49055) and *Cha3.3kbp-Gal80*[54] (gift from Dr. Toshihiro Kitamoto))

588

589 **Calcium imaging**

590 The larvae were dissected and their CNSs were isolated and placed on a MAS-coated slide glass
591 (S9215, Matsunami Glass, Japan) in TES buffer (TES 5 mmol, NaCl 135 mmol, KCl 5 mmol,
592 $CaCl_2$ 2 mmol, $MgCl_2$ 4 mmol, Sucrose 36 mmol). The imaging was conducted with an EMCCD
593 camera (iXon, ANDOR TECHNOLOGY, UK) mounted on an upright microscope (Axioskop2 FS,
594 Zeiss, Germany) equipped with a spinning-disk confocal unit (CSU21, Yokogawa, Japan) and a
595 20X water immersion objective lens (UMPlanFLN 20XW, Olympus, Japan). In experiments with
596 GCaMP6s or GCaMP6f, 488 nm blue light (CSU-LS2WF, Solution Systems, Japan) with an
597 intensity of 4.5 μW/mm$^2$ was used. The light intensity was measured by the laser power meter
598 (LP1, Sanwa Electric Instrument, Japan). Exposure time and frequency (frames per second, fps)

were 99.1 ms and 10 fps for imaging of Canon neurons (Fig. 1b and 6g, h), 50 ms and 6 fps for simultaneous imaging of aCC MNs and Canon neurons (Fig. 1c, d, and Supplementary Fig. 1e), and 85 ms and 5fps for simultaneous imaging of aCC MNs and GVLIs (Supplementary Fig. 4f). To rapidly acquire images from two focal planes each containing aCC MNs and Canon neurons or aCC MNS and GVLIs, a piezo unit (P-725, Physik Instrumente, Germany) controlled by a piezo Z controller (E-665 Piezo Amplifier/Servo Controller, Physik Instrumente, Germany) and a precise control unit (ER-PCUA-100, ANDOR TECHNOLOGY, UK) was used.

The regions of interest (ROIs) were set to surround the axons or cell bodies of the target neurons. Signal intensity in each frame was defined as the maximum or mean signal value among all pixels within each ROI. After extraction of raw signal data, a Savitzky-Golay filter was applied to the raw data to remove noise and perform smoothing. The calcium signals were normalized by the baseline intensity as follows,

$$\frac{\Delta F}{F} = \frac{F_{ROI[n]}(t) - Fb_{ROI[n]}(t)}{Fb_{ROI[n]}(t)}$$

where $n$ designates the ROI identity, $t$ the frame number, $F_{ROI[n]}(t)$ the signal intensity at $t$, and $Fb_{ROI[n]}(t)$ baseline intensity defined as the minimum $F_{ROI[n]}(t)$ between $t$ to $t + 100$. In order to focus on and visualize the neural activity timing of A02e and A31k (Supplementary Fig. 7f, g), the signal of each neuron, $\frac{\Delta F}{F}$, was normalized at its maximum value to obtain the normalized signal, $\frac{\Delta F}{F}_{norm}$.

## Analysis of phase lag during fictive locomotion

To evaluate the time lag between the activity of aCC MNs and Canon neurons (Fig. 1d, and Supplementary Fig. 1e), we focused on the initiation and peak of the rise in calcium signals in each fictive backward locomotion. The initiation was defined as the time when a rise in fluorescent started before the peak. For the analysis of activity timing of Canon and aCC MNs (Fig. 1d), peak time for neuron $X$ ( $X =$

$\{aCCA2, aCCA3, aCCA4, aCCA5, aCCA6, CanonA3, CanonA4, CanonA5\}$), $t_{P_X}$, was normalized to the duration of wave propagation from A2 to A6 aCC MNs to give $t_{P_{Xnorm}}$ as follows.

$$t_{P_{Xnorm}} = \frac{t_{P_X} - t_{P_{aCCA2}}}{t_{P_{aCCA6}} - t_{P_{aCCA2}}}$$

For the analysis of activity duration of Canon and aCC neurons (Supplementary Fig. 1e), initiation time ($t_{I_X}$) for neuron $X$ was also normalized to give $t_{I_{Xnorm}}$ as follow.

$$t_{I_{Xnorm}} = \frac{t_{I_X} - t_{I_{aCCA2}}}{t_{P_{aCCA6}} - t_{I_{aCCA2}}}$$

For the analysis of activity duration of A31k and A02e (Supplementary Fig. 7h), we used the data obtained in a previous research[24], in which GCaMP6f signals of A31k and A02e were recorded simultaneously with RGECO1 signals of A02e as a reference. Here normalized activity duration of A02e or A31k recorded with GCaMP6f located in A3 neuromere, $\tau_X$, is defined by the following equation.

$$\tau_X = \frac{t_{P_X} - t_{I_X}}{t_{P_{A02eRGECO1}} - t_{I_{A02eRGECO1}}}$$

## Immunohistochemistry

The larvae were pinned on a silicon-filled dish and dissected in TES buffered saline. After dissection, the larvae were rinsed with phosphate buffered saline (PBS) and fixed in 4 % paraformaldehyde in PBS for 30 min at room temperature. After a 30 min rinse with 0.2 % Triton X-100 in PBS (PBT), the larvae were incubated with 5 % normal goat serum (NGS) in PBT for 30 min. Then the larvae were incubated for at least 18 hours at 4 °C with the primary antibodies mixed in with 5 % NGS in PBT. After a 30 min rinse, the larvae were incubated at 4 °C with the secondary antibodies mixed in with 5 % NGS in PBT for at least 12 hours. Fluorescent images

were scanned and acquired using a confocal microscope (FV1000, Olympus, Japan) with a 20X water immersion objective lens (UMPlanFLN 20XW, Olympus, Japan) or a 100X water immersion objective lens (LUMPlanFl 100XW, Olympus, Japan). Antibodies: rabbit anti-GFP (Af2020, Frontier Institute; 1:1000; RRID: AB 2571573), guinea pig anti-GFP (Af1180, Frontier Institute; 1:1000; RRID: AB 2571575), mouse anti-FasII (1D4, Hybridoma Bank (University of Iowa); 1:10; RRID: AB 528235), rabbit anti-HA (C29F4, Cell Signaling Technology; 1:300; RRID: AB 1549585), rat anti-FLAG (NBP1-06712, Novus Biologicals; 1:200; RRID: AB 1625981), mouse anti-ChAT (4B1, Hybridoma Bank (University of Iowa); 1:50; RRID: AB 528122), rabbit anti-GABA (A2052, Sigma; 1:100; RRID: AB 477652), rabbit anti-vGluT (Gift from Dr. Hermann Aberle; 1:1000; RRID: AB 2315544), mouse anti-Brunchpilot (Brp) (nc82, Hybridoma Bank (University of Iowa); 1:50; RRID: AB 2314866), goat Alexa Fluor 488 anti-rabbit (A11034, Thermo Fisher Scientific; 1:300; RRID AB 2576217), goat Cy3 anti-rabbit (A10520, Thermo Fisher Scientific; 1:300; RRID: AB 10563288), goat Cy5 anti-rabbit (A10523, Thermo Fisher Scientific; 1:300; RRID: AB 2534032), goat Alexa Fluor 555 anti-mouse (A21424, Thermo Fisher Scientific; 1:300; RRID: AB 141780), goat Cy5 anti-mouse (A10524, Thermo Fisher Scientific; 1:300; RRID: AB 2534033), goat Alexa Fluor 633 anti-rat (A21094, Thermo Fisher Scientific; 1:300; RRID: AB 141553), goat Alexa Fluor 488 anti-guinea pig (A11073, Thermo Fisher Scientific; 1:300; RRID: AB 2534117), goat Alexa Fluor 647 anti-Horseradish Peroxidase (HRP) (123-605-021, Jackson ImmunoResearch; 1:200; RRID: AB 2338967)

## Optogenetics in behaving larvae

In this study, CsChrimson[32] and GtACR1[41] was used for optogenetical activation and inactivation of neurons, respectively. The larvae were grown at 25 °C in vials with food, either containing 1 mmol of all-trans retinal (ATR) or none. The vials were covered with aluminum foil. Third instar larvae were gathered and washed to remove extraneous matter. Each behavior assay was conducted on an agar plate under shaded conditions. The surface temperature was adjusted at 25 °C ±1 °C by a heating plate and the room temperature was also set at 25 °C ±1 °C. For

677 optogenetic activation with CsChimrson, red LED light (660 nm LED, THORLABS, USA) was
678 applied with an intensity of 250 μW/mm$^2$ while larvae were performing sequential forward
679 locomotion. For optogenetic inhibition with GtACR1, green light (530-550 nm) from a lamp (X-
680 Cite, Olympus, Japan) with RFP1 filter was applied with an intensity of 1 mW/mm$^2$. The light
681 intensity was measured using a laser power meter (LP1, Sanwa Electric Instrument, Japan). Trials
682 with a duration of five seconds were applied once for each animal. The intensity of the background
683 illumination was set as low as possible so as not to activate CsChrimson or GtACR1. A CCD
684 camera (XCD-V60, SONY, Japan) under a stereo-microscope (SZX16, Olympus, Japan) was
685 used for recording larval behavior. For quantification with CsChrimson, we counted the number
686 of forward peristalses performed in the first two seconds after light stimulation onset in each trial.
687

688 **Imaging and quantification of muscular movements**

689 The larvae were pinned on a silicon-filled dish and dissected along the dorsal side in TES buffered
690 saline then the larval internal tissues were removed. In the experiment with Kir (Fig. 3 and
691 Supplementary Fig. 2c, d), a lamp (X-Cite, Olympus, Japan) was used as a light source to
692 illuminate the muscles at a light density of 7 μW/mm$^2$. To quantitate muscular contraction and
693 relaxation, we manually measured the length of muscle 6 in segment A3, $L_{raw}(t)$ , in each frame
694 during the recordings, using an annotation tool we developed that records the xy coordinate of a
695 point clicked in a frame and calculates the distance between clicked points. The Savitzky-Golay
696 filter was applied to the data to remove noise. We designated the frame number by $t$ and muscular
697 length by a function of $t$, $L(t)$. $L(\tau)$ was provided as a value of $t = \tau$ of an approximate curve
698 approximated to the data of $L_{raw}(t)$ within range $[\tau - 10, \tau + 10]$. $L(t)$ was differentiable and we
699 defined the maximum relaxation speed (Fig. 3e, f) as the maximum time differential of $L(t)$ during
700 muscle relaxation and maximum contraction speed (Fig. 3g, h) as the absolute value of the
701 minimum time differential of $L(t)$ during muscle contraction. The duration of muscular contraction
702 (Fig. 3i, j) was defined as the period from initiation of contraction to termination of relaxation.
703

## EM reconstruction using CATMAID

Acquisition and analysis of ssTEM data are described in previous researches[26,37,46]. We manually traced axons, dendrites, presynaptic sites (identified by the presence of a T-bar) and postsynaptic sites of Canon and other neurons using CATMAID[35] (annotated in CATMAID as "A18g").

## Analysis of activity propagation in Canon-Canon network

To evaluate the effect of TeTxLC expressed in Canon neurons on their activity propagation, we defined “complete” and “incomplete” peristalses waves as follows. A complete wave was defined as a wave in which Canon activities in all neuromeres examined were high ( $\frac{\Delta F}{F}$ in each neuron at the peak is more than half of the maximum value of $\frac{\Delta F}{F}$ during the recording). An incomplete wave was defined as a wave in which more than one Canon neuron showed low-level neural activity ($\frac{\Delta F}{F}$ at the peak is less than half of the maximum value of $\frac{\Delta F}{F}$).

## Statistical Analysis

The two-sided Mann-Whitney U test, the two-sided Fisher's exact test, or Chi-squared test were used to determine statistical significance as indicated in Figure legends. In multiple comparisons, the Holm method was used to avoid the family-wise error. The sample sizes are indicated within the respective figure as "$n$".

All statistical tests and quantification were performed using Python3.

# References

1. Pearson, K. G. Common Principles of Invertebrates. *Annu. Rev. Neurosci.* **16**, 265–97 (1993).
2. Marder, E. & Calabrese, R. L. Principles of rhythmic motor pattern generation. *Physiol. Rev.* **76**, 687–717 (1996).
3. Grillner, S. Neurobiological bases of rhythmic motor acts in vertebrates. *Science (80-. ).*

**228**, 143–149 (1985).

4. Gowda, S. B. M. *et al.* GABAergic inhibition of leg motoneurons is required for normal walking behavior in freely moving Drosophila. *Proc. Natl. Acad. Sci. U. S. A.* **115**, E2115–E2124 (2018).

5. Kohsaka, H., Takasu, E., Morimoto, T. & Nose, A. A group of segmental premotor interneurons regulates the speed of axial locomotion in drosophila larvae. *Curr. Biol.* **24**, 2632–2642 (2014).

6. Goulding, M., Bourane, S., Garcia-Campmany, L., Dalet, A. & Koch, S. Inhibition downunder: an update from the spinal cord. *Curr. Opin. Neurobiol.* **26**, 161–166 (2014).

7. Britz, O. *et al.* A genetically defined asymmetry underlies the inhibitory control of flexor–extensor locomotor movements. *Elife* **4**, 1–22 (2015).

8. Kato, K., Vogt, T. & Kanosue, K. Brain Activity Underlying Muscle Relaxation. *Front. Physiol.* **10**, (2019).

9. Grasso, M., Mazzini, L. & Schieppati, M. Muscle relaxation in Parkinson's disease: A reaction time study. *Mov. Disord.* **11**, 411–420 (1996).

10. Machuca-Tzili, L., Brook, D. & Hilton-Jones, D. Clinical and molecular aspects of the myotonic dystrophies: A review. *Muscle and Nerve* **32**, 1–18 (2005).

11. Wiens, T. J. & Wolf, H. The inhibitory motoneurons of crayfish thoracic limbs: Identification, structures, and homology with insect common inhibitors. *J. Comp. Neurol.* **336**, 261–278 (1993).

12. Bräunig, P., Schmäh, M. & Wolf, H. Common and specific inhibitory motor neurons innervate the intersegmental muscles in the locust thorax. *J. Exp. Biol.* **209**, 1827–1836 (2006).

13. Gao, S. & Zhen, M. Action potentials drive body wall muscle contractions in Caenorhabditis elegans. *Proc. Natl. Acad. Sci. U. S. A.* **108**, 2557–2562 (2011).

14. Grillner, S. & Jessell, T. M. Measured motion: searching for simplicity in spinal locomotor networks. *Curr. Opin. Neurobiol.* **19**, 572–586 (2009).

15. Kiehn, O. Decoding the organization of spinal circuits that control locomotion. *Nat. Rev. Neurosci.* **17**, 224–238 (2016).

16. Kohsaka, H., Guertin, P. A. & Nose, A. Neural Circuits Underlying Fly Larval Locomotion. *Curr. Pharm. Des.* **23**, 1722–1733 (2017).

17. Clark, M. Q., Zarin, A. A., Carreira-Rosario, A. & Doe, C. Q. Neural circuits driving larval locomotion in Drosophila. *Neural Dev.* **13**, 1–10 (2018).

18. Kohsaka, H., Okusawa, S., Itakura, Y., Fushiki, A. & Nose, A. Development of larval motor circuits in Drosophila. *Dev. Growth Differ.* **54**, 408–419 (2012).

19. Xiang, Y. *et al.* Light-avoidance-mediating photoreceptors tile the Drosophila larval body wall. *Nature* **468**, 921–926 (2010).

20. Takagi, S. *et al.* Divergent Connectivity of Homologous Command-like Neurons Mediates Segment-Specific Touch Responses in Drosophila. *Neuron* **96**, 1373-1387.e6 (2017).

21. Heckscher, E. S., Lockery, S. R. & Doe, C. Q. Characterization of Drosophila larval crawling at the level of organism, segment, and somatic body wall musculature. *J. Neurosci.* **32**, 12460–12471 (2012).

22. Gjorgjieva, J., Berni, J., Evers, J. F. & Eglen, S. J. Neural circuits for peristaltic wave propagation in crawling Drosophila larvae: analysis and modeling. *Front. Comput. Neurosci.* **7**, 1–19 (2013).

23. Heckscher, E. S. *et al.* Even-Skipped+ Interneurons Are Core Components of a Sensorimotor Circuit that Maintains Left-Right Symmetric Muscle Contraction Amplitude. *Neuron* **88**, 314–329 (2015).

24. Kohsaka, H. *et al.* Regulation of forward and backward locomotion through intersegmental feedback circuits in Drosophila larvae. *Nat. Commun.* **10**, 1–11 (2019).

25. Fushiki, A. *et al.* A circuit mechanism for the propagation of waves of muscle contraction in Drosophila. *Elife* **5**, 1–23 (2016).

26. Ohyama, T. *et al.* A multilevel multimodal circuit enhances action selection in Drosophila. *Nature* **520**, 633–639 (2015).

27. Pulver, S. R. *et al.* Imaging fictive locomotor patterns in larval Drosophila. *J. Neurophysiol.* **114**, 2564–2577 (2015).

28. Park, J., Kondo, S., Tanimoto, H., Kohsaka, H. & Nose, A. Data-driven analysis of motor activity implicates 5-HT2A neurons in backward locomotion of larval Drosophila. *Sci. Rep.* **8**, 10307 (2018).

29. Nern, A., Pfeiffer, B. D. & Rubin, G. M. Optimized tools for multicolor stochastic labeling reveal diverse stereotyped cell arrangements in the fly visual system. *Proc. Natl. Acad. Sci. U. S. A.* **112**, E2967–E2976 (2015).

30. Nicolaï, L. J. J. *et al.* Genetically encoded dendritic marker sheds light on neuronal connectivity in Drosophila. *Proc. Natl. Acad. Sci. U. S. A.* **107**, 20553–20558 (2010).

31. Mahr, A. & Aberle, H. The expression pattern of the Drosophila vesicular glutamate transporter: A marker protein for motoneurons and glutamatergic centers in the brain. *Gene Expr. Patterns* **6**, 299–309 (2006).

32. Klapoetke, N. C. *et al.* Independent optical excitation of distinct neural populations. *Nat. Methods* **11**, 338–346 (2014).

33. R. C. Hardie, P. R. Calcium influx via TRP channels is required to maintain PIP. *Neuron* **30**, 149–59 (2001).

34. Hughes, C. L. & Thomas, J. B. A sensory feedback circuit coordinates muscle activity in Drosophila. *Mol. Cell. Neurosci.* **35**, 383–396 (2007).

35. Saalfeld, S., Cardona, A., Hartenstein, V. & Tomančák, P. CATMAID: Collaborative annotation toolkit for massive amounts of image data. *Bioinformatics* **25**, 1984–1986 (2009).

36. Carreira-Rosario, A. *et al.* MDN brain descending neurons coordinately activate backward and inhibit forward locomotion. *Elife* **7**, (2018).

37. Schneider-Mizell, C. M. *et al.* Quantitative neuroanatomy for connectomics in Drosophila. *Elife* **5**, 1–36 (2016).

38. Zarin, A. A., Mark, B., Cardona, A., Litwin-Kumar, A. & Doe, C. Q. A multilayer circuit

architecture for the generation of distinct locomotor behaviors in Drosophila. *Elife* **8**, 1–34 (2019).

39. Itakura, Y. *et al.* Identification of inhibitory premotor interneurons activated at a late phase in a motor cycle during drosophila larval locomotion. *PLoS One* **10**, 1–24 (2015).

40. Sales, E. C., Heckman, E. L., Warren, T. L. & Doe, C. Q. Regulation of subcellular dendritic synapse specificity by axon guidance cues. *Elife* **8**, (2019).

41. Mohammad, F. *et al.* Optogenetic inhibition of behavior with anion channelrhodopsins. *Nat. Methods* **14**, 271–274 (2017).

42. Sweeney, S. T., Broadie, K., Keane, J., Niemann, H. & O'Kane, C. J. Targeted expression of tetanus toxin light chain in Drosophila specifically eliminates synaptic transmission and causes behavioral defects. *Neuron* **14**, 341–351 (1995).

43. Wolf, H. Activity patterns of inhibitory motoneurones and their impact on leg movement in tethered walking locusts. *J. Exp. Biol.* **152**, 281–304 (1990).

44. Thapliyal, S. & Babu, K. C. elegans locomotion: Finding balance in imbalance. in *Advances in Experimental Medicine and Biology* (2018). doi:10.1007/978-981-13-3065-0_14.

45. Landgraf, M., Bossing, T., Technau, G. M. & Bate, M. The origin, location, and projections of the embryonic abdominal motorneurons of Drosophila. *J. Neurosci.* **17**, 9642–9655 (1997).

46. Zwart, M. F. *et al.* Selective Inhibition Mediates the Sequential Recruitment of Motor Pools. *Neuron* **91**, 615–628 (2016).

47. Crapse, T. B. & Sommer, M. A. Corollary discharge across the animal kingdom. *Nat. Rev. Neurosci.* **9**, 587–600 (2008).

48. Vaadia, R. D. *et al.* Characterization of Proprioceptive System Dynamics in Behaving Drosophila Larvae Using High-Speed Volumetric Microscopy. *Curr. Biol.* **29**, 935-944.e4 (2019).

49. Landgraf, M., Sánchez-Soriano, N., Technau, G. M., Urban, J. & Prokop, A. Charting the

838 Drosophila neuropile: A strategy for the standardised characterisation of genetically
839 amenable neurites. *Dev. Biol.* **260**, 207–225 (2003).
840 50. Fujioka, M. Even-skipped, acting as a repressor, regulates axonal projections in
841 Drosophila. *Development* **130**, 5385–5400 (2003).
842 51. Chen, T. W. *et al.* Ultrasensitive fluorescent proteins for imaging neuronal activity. *Nature*
843 **499**, 295–300 (2013).
844 52. Han, C., Jan, L. Y. & Jan, Y. N. Enhancer-driven membrane markers for analysis of
845 nonautonomous mechanisms reveal neuron-glia interactions in Drosophila. *Proc. Natl.*
846 *Acad. Sci. U. S. A.* **108**, 9673–9678 (2011).
847 53. Macpherson, L. J. *et al.* Dynamic labelling of neural connections in multiple colours by
848 trans-synaptic fluorescence complementation. *Nat. Commun.* **6**, 1–9 (2015).
849 54. Kitamoto, T. Conditional disruption of synaptic transmission induces male-male courtship
850 behavior in Drosophila. *Proc. Natl. Acad. Sci. U. S. A.* **99**, 13232–13237 (2002).
851

Fig. 1

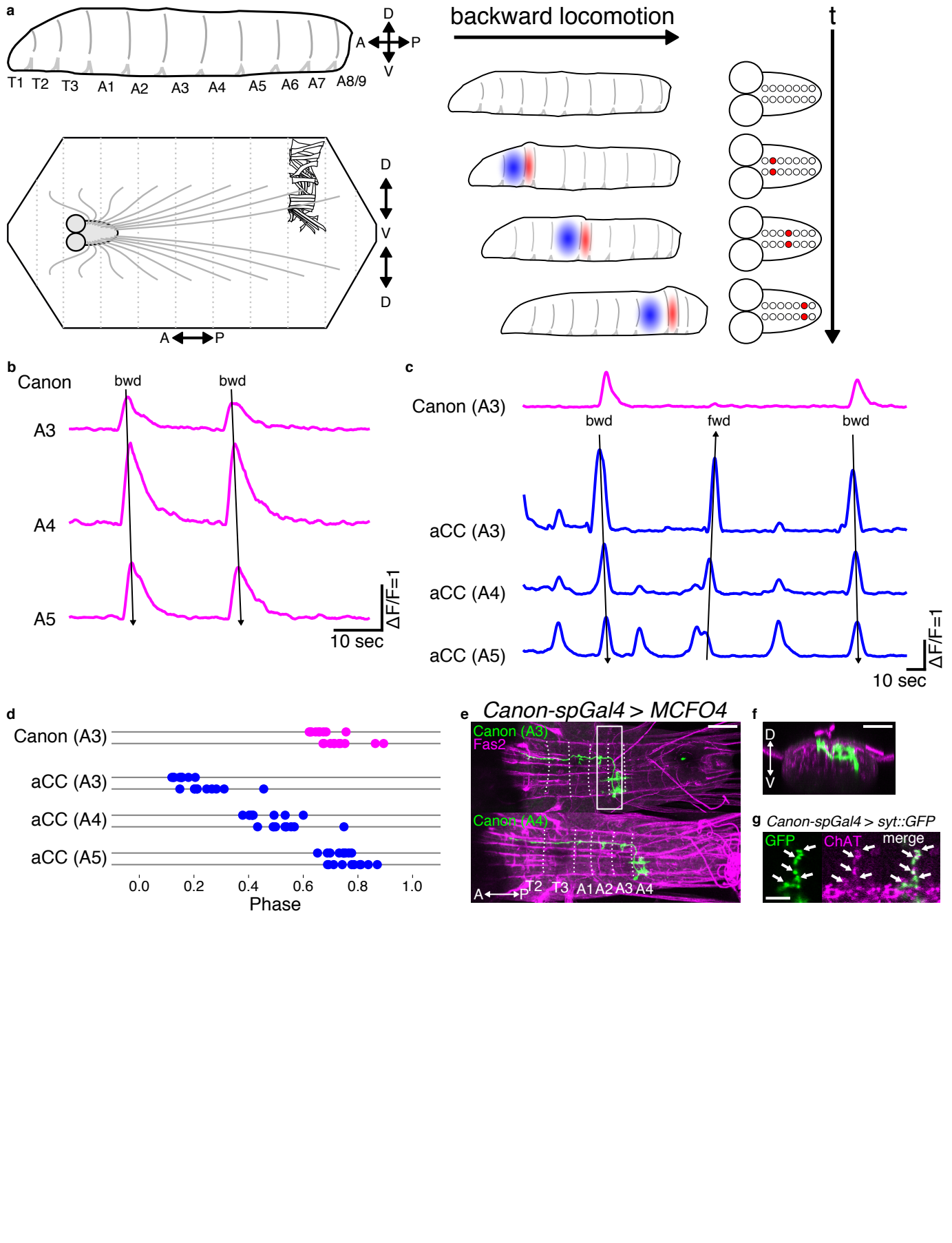
a
T1 T2 T3 A1 A2 A3 A4 A5 A6 A7 A8/9
D
A
P
V
backward locomotion
t
b
Canon
bwd
bwd
A3
A4
A5
10 sec
ΔF/F=1
c
Canon (A3)
bwd
fwd
bwd
aCC (A3)
aCC (A4)
aCC (A5)
10 sec
ΔF/F=1
d
Canon (A3)
aCC (A3)
aCC (A4)
aCC (A5)
0.0
0.2
0.4
0.6
0.8
1.0
Phase
e
Canon-spGal4 > MCFO4
Canon (A3)
Fas2
Canon (A4)
A
P
T2 T3 A1 A2 A3 A4
f
D
V
g
Canon-spGal4 > syt::GFP
GFP
ChAT
merge

Fig. 2

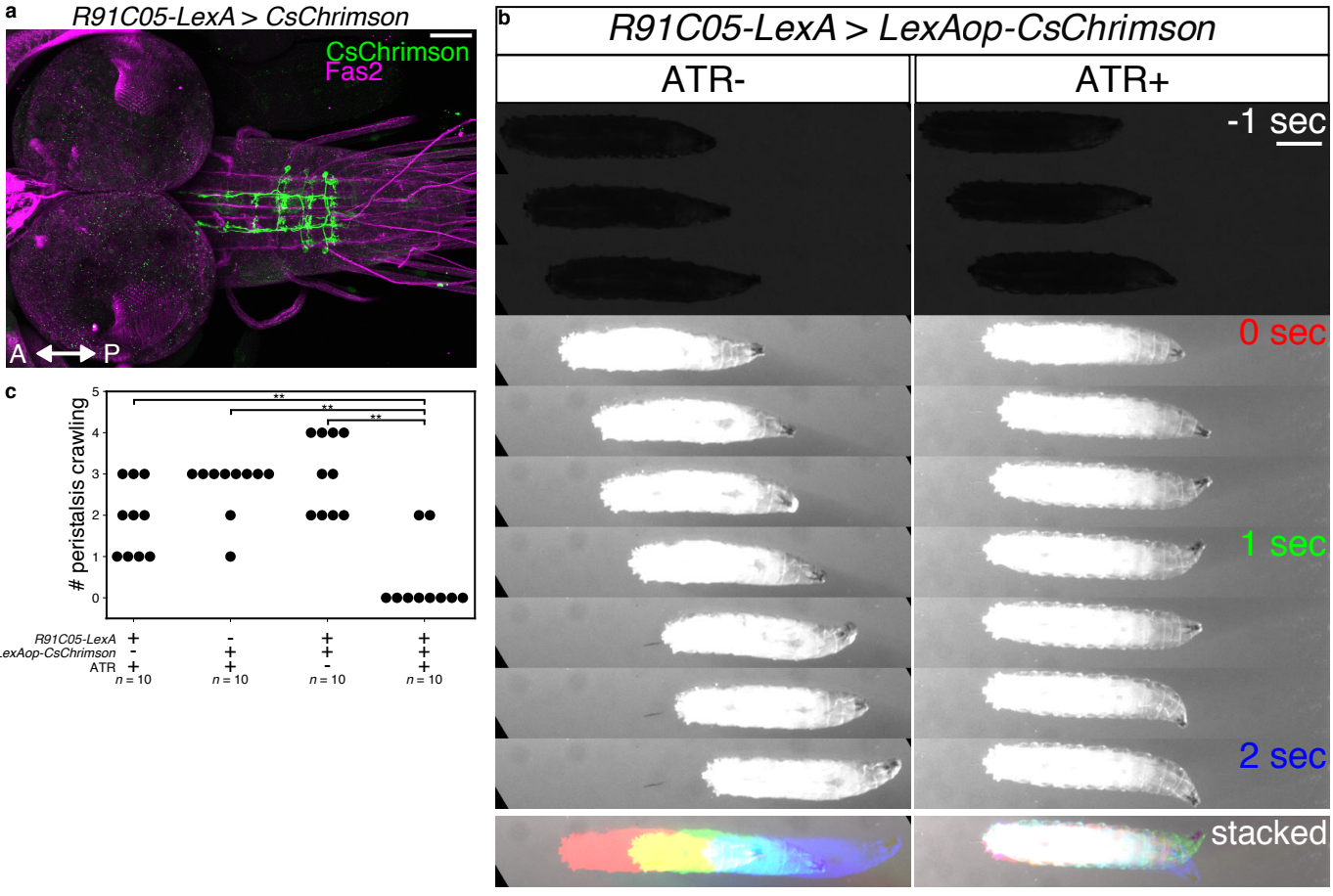
a
R91C05-LexA > CsChrimson
CsChrimson
Fas2
A
P
b
R91C05-LexA > LexAop-CsChrimson
ATR-
ATR+
-1 sec
0 sec
1 sec
2 sec
stacked
c
# peristalsis crawling
0
1
2
3
4
5
**
**
**
R91C05-LexA + - + +
LexAop-CsChrimson - + + +
ATR + + - +
n = 10
n = 10
n = 10
n = 10

Fig. 3

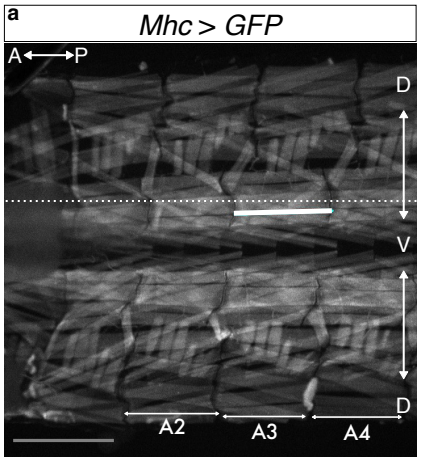
a
Mhc > GFP
A
P
D
V
D
A2
A3
A4

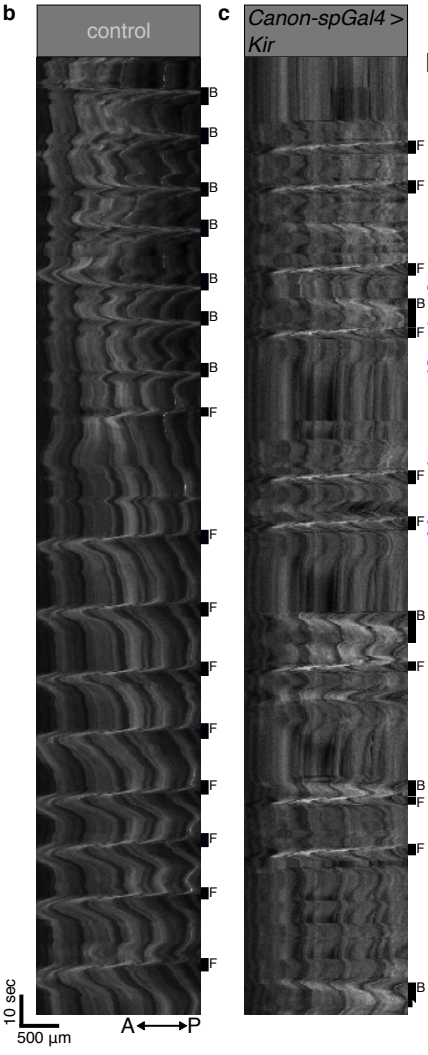
b
control
c
Canon-spGal4 > Kir
B
F
10 sec
500 µm
A
P

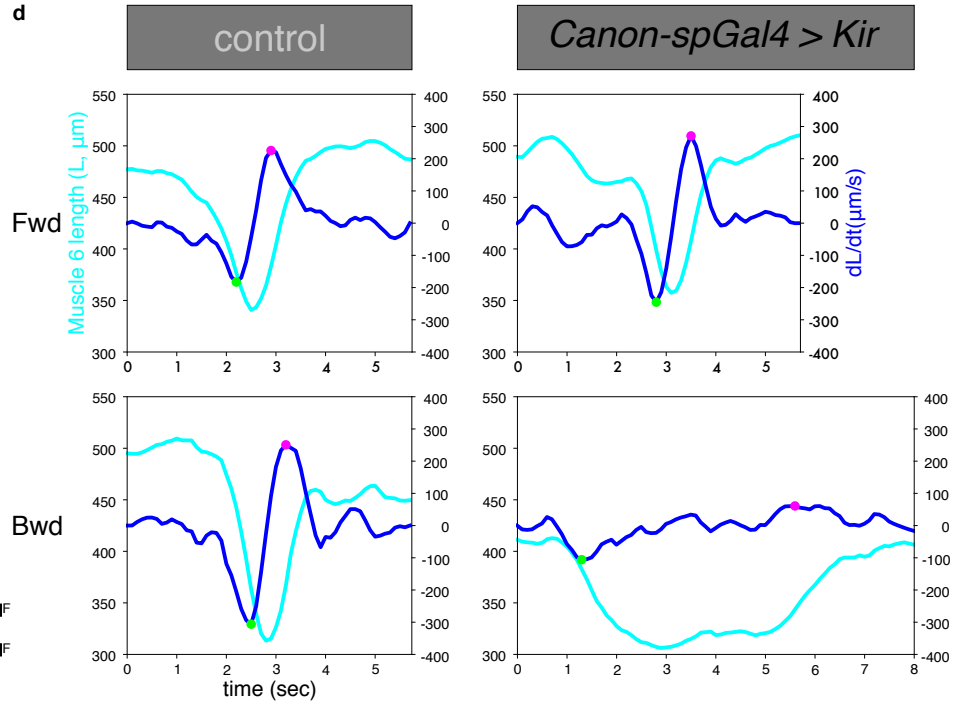
d
control
Canon-spGal4 > Kir
Fwd
Bwd
Muscle 6 length (L, µm)
dL/dt(µm/s)
time (sec)

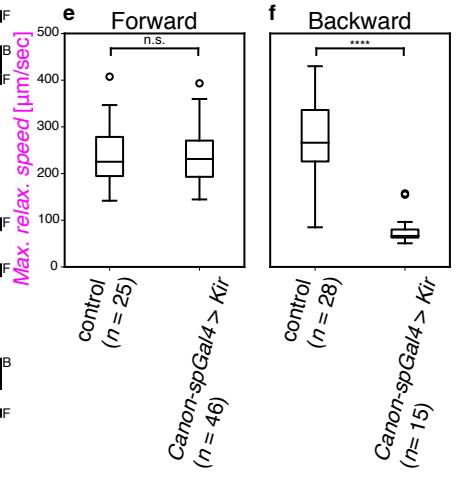
e
Forward
n.s.
Max. relax. speed [µm/sec]
control (n = 25)
Canon-spGal4 > Kir (n = 46)


f
Backward
****
control (n = 28)
Canon-spGal4 > Kir (n= 15)

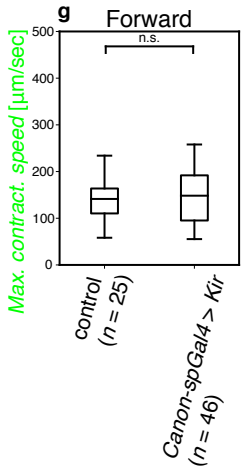
g
Forward
n.s.
Max. contract. speed [µm/sec]
control (n = 25)
Canon-spGal4 > Kir (n = 46)

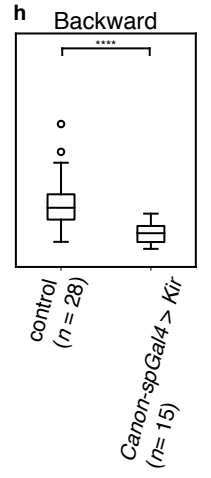
h
Backward
****
control (n = 28)
Canon-spGal4 > Kir (n= 15)

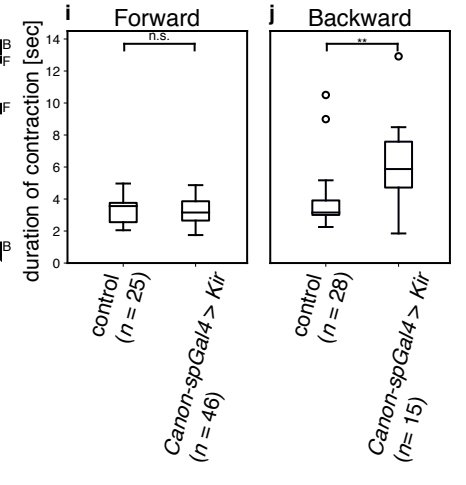
i
Forward
n.s.
duration of contraction [sec]
control (n = 25)
Canon-spGal4 > Kir (n = 46)


j
Backward
**
control (n = 28)
Canon-spGal4 > Kir (n= 15)

Fig. 4

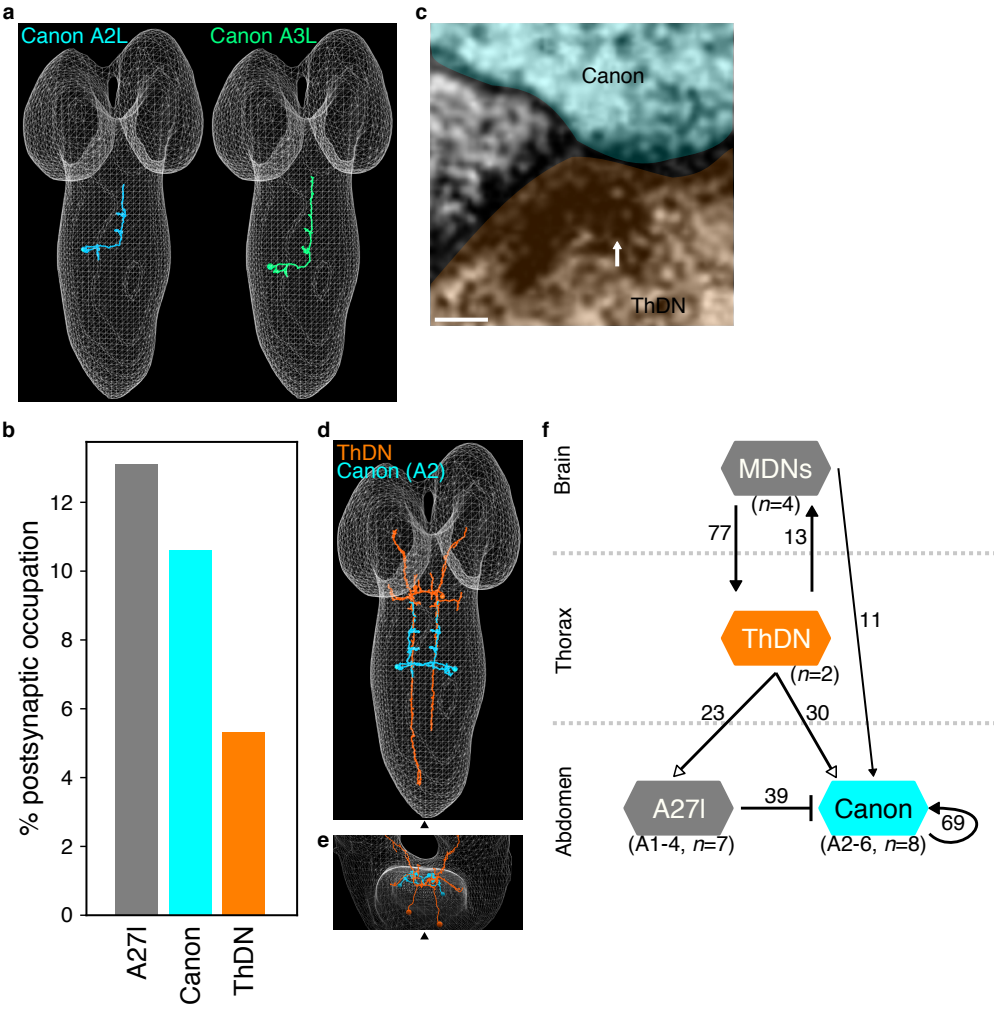
a
Canon A2L
Canon A3L
c
Canon
ThDN
b
% postsynaptic occupation
0
2
4
6
8
10
12
A27l
Canon
ThDN
d
ThDN
Canon (A2)
e
f
Brain
Thorax
Abdomen
MDNs
(n=4)
77
13
11
ThDN
(n=2)
23
30
A27l
(A1-4, n=7)
39
Canon
(A2-6, n=8)
69

Fig.5

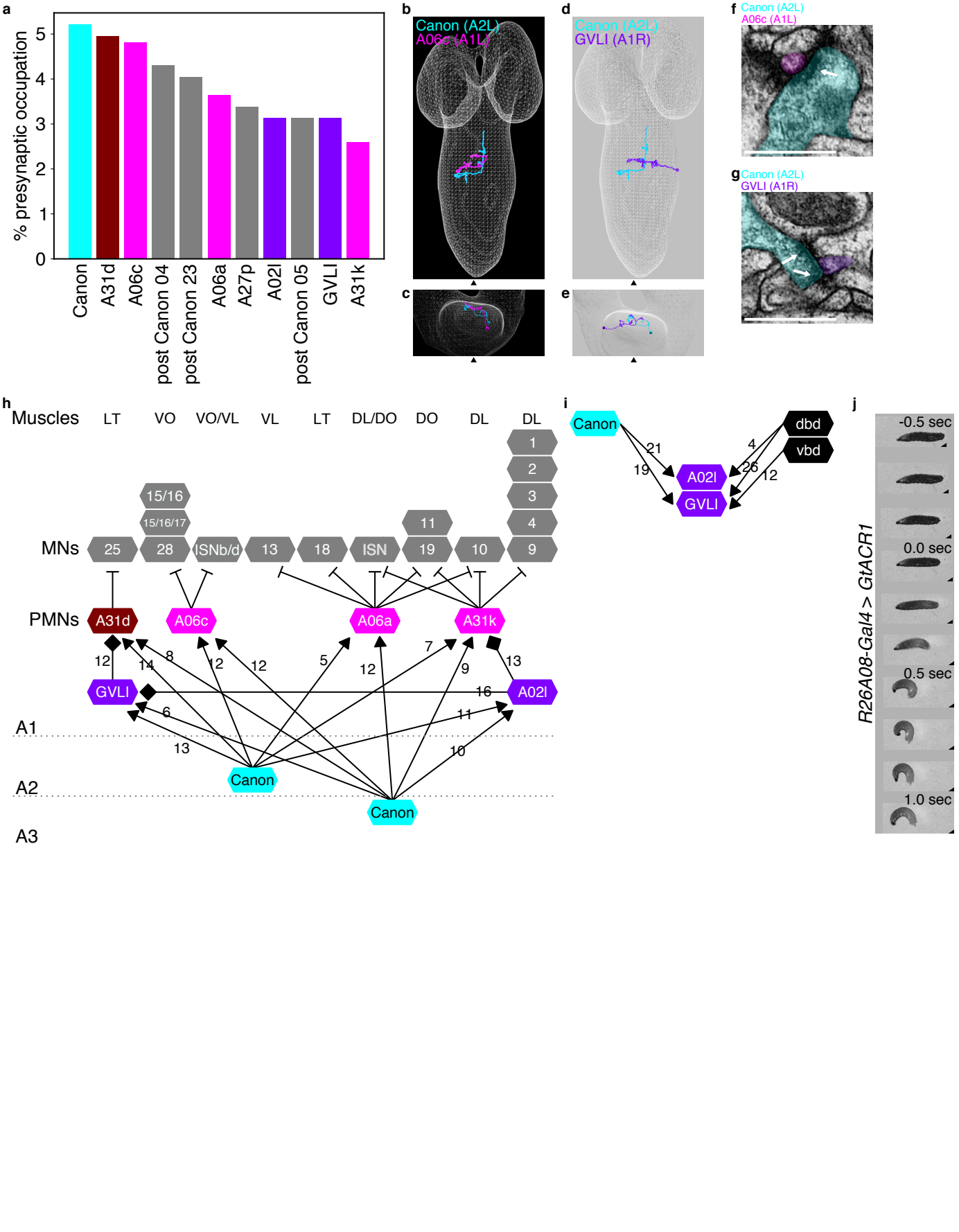
a
% presynaptic occupation
0
1
2
3
4
5
Canon
A31d
A06c
post Canon 04
post Canon 23
A06a
A27p
A02l
post Canon 05
GVLl
A31k
b
Canon (A2L)
A06c (A1L)
c
d
Canon (A2L)
GVLl (A1R)
e
f
Canon (A2L)
A06c (A1L)
g
Canon (A2L)
GVLl (A1R)
h
Muscles
LT
VO
VO/VL
VL
LT
DL/DO
DO
DL
DL
1
2
3
4
11
15/16
15/16/17
MNs
25
28
ISNb/d
13
18
ISN
19
10
9
PMNs
A31d
A06c
A06a
A31k
12
14
8
12
12
5
12
7
9
13
GVLl
16
A02l
6
11
13
10
A1
A2
A3
Canon
Canon
i
Canon
21
19
A02l
GVLl
4
26
12
dbd
vbd
j
R26A08-Gal4 > GtACR1
-0.5 sec
0.0 sec
0.5 sec
1.0 sec

Fig.6

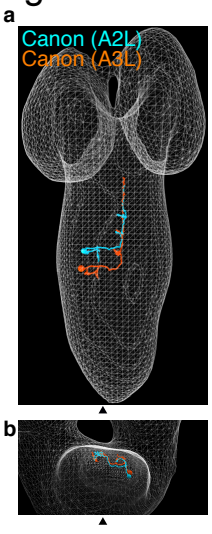


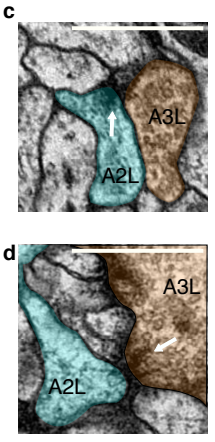


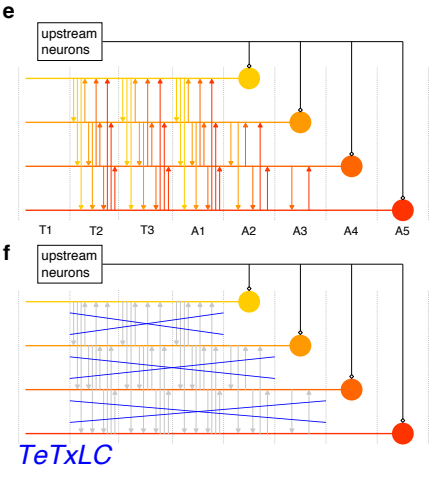


i

| | -TeTxLC | +TeTxLC |
|---|---|---|
| complete | 19 | 14 |
| incomplete | 0 | 13 |

$^{***}p = 3.56\text{x}10^{-4}$

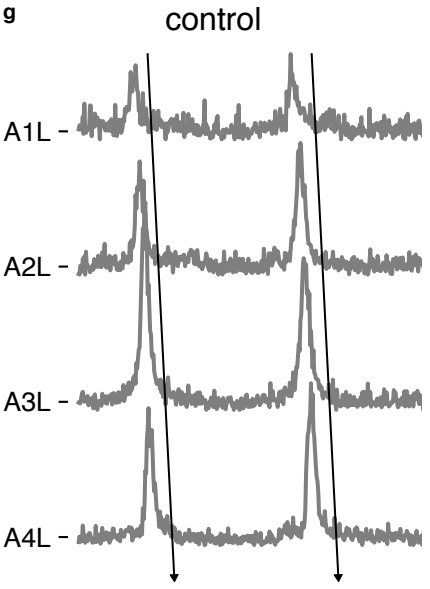


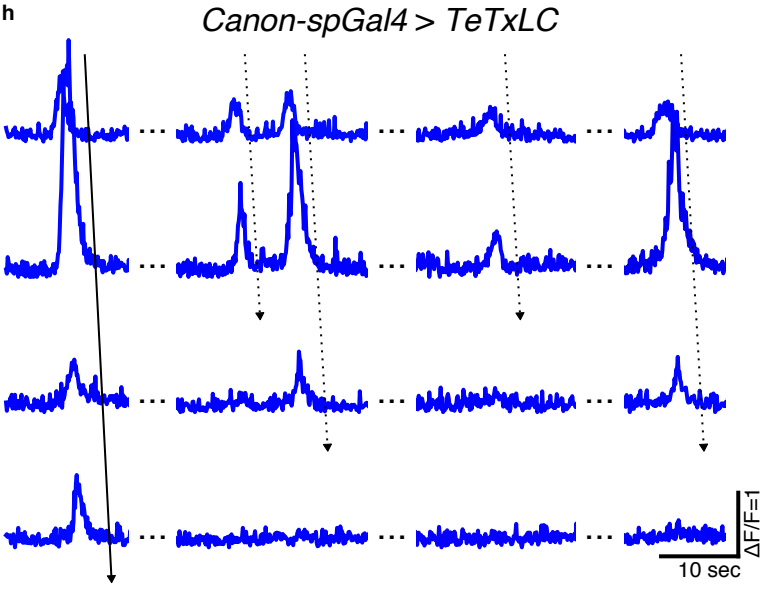

Fig. 7

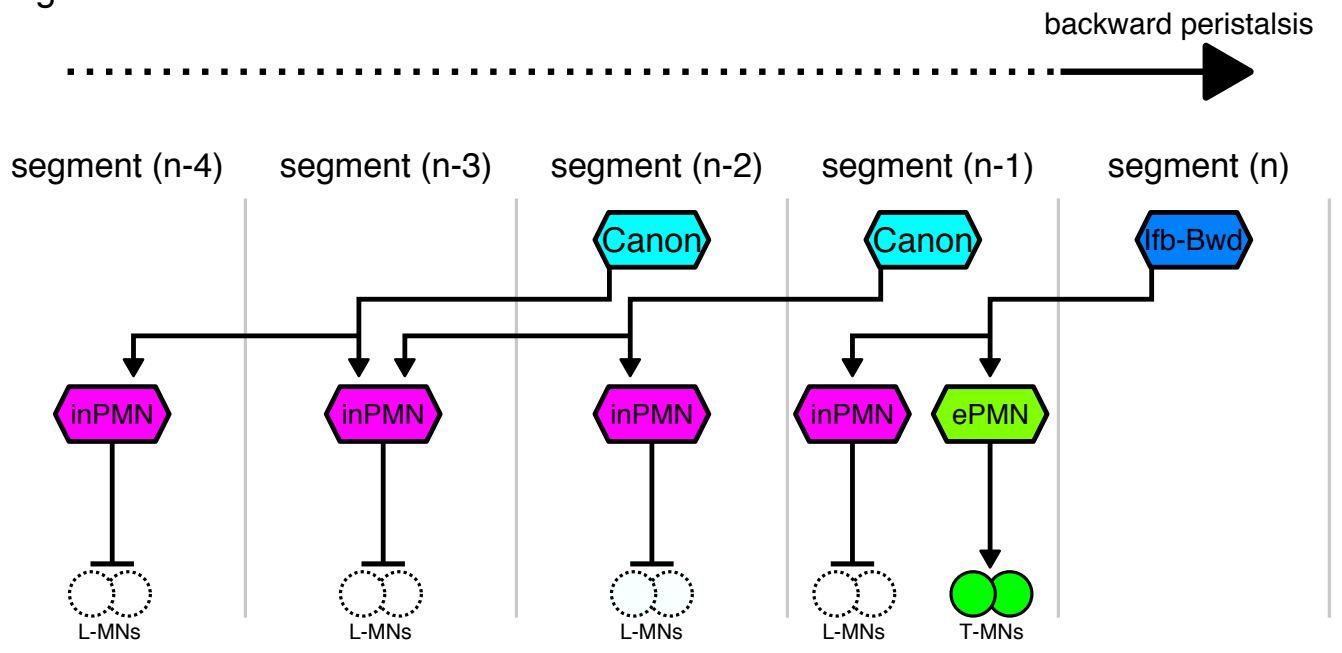
backward peristalsis
segment (n-4)
segment (n-3)
segment (n-2)
segment (n-1)
segment (n)
Canon
Canon
lfb-Bwd
inPMN
inPMN
inPMN
inPMN
ePMN
L-MNs
L-MNs
L-MNs
L-MNs
T-MNs